Frauenfelder, H., Petsko, G. A., & Tsernoglou, D. (1979) *Nature (London) 280*, 558–563.
Gelin, B. R., & Karplus, M. (1975) *Proc. Natl. Acad. Sci. U.S.A. 72*, 2002–2006.
Gurd, F. R. N., & Rothgeb, T. M. (1979) *Adv. Protein Chem. 33*, 73–165.
Karplus, M., & McCammon, J. A. (1979) *Nature (London) 277*, 578.
Karplus, M., & McCammon, J. A. (1981) *CRC Crit. Rev. Biochem. 9*, 293–349.
Konnert, J. H., & Hendrickson, W. A. (1980) *Acta Crystallogr., Sect. A A36*, 344–350.
Kushick, J., & Berne, B. J. (1977) *Mod. Theor. Chem. 6*, 41–63.
Levy, R. M., & Karplus, M. (1979) *Biopolymers 18*, 2465–2495.
Levy, R. M., Karplus, M., & McCammon, J. A. (1981a) *J. Am. Chem. Soc. 103*, 994–996.
Levy, R. M., Karplus, M., & Wolynes, P. G. (1981b) *J. Am. Chem. Soc. 103*, 5998–6011.
Levy, R. M., Perahia, D., & Karplus, M. (1982) *Proc. Natl. Acad. Sci. U.S.A. 79*, 1346–1350.
Mao, B., Pear, M. R., McCammon, J. A., & Northrup, S. H. (1982) *Biopolymers* (in press).
McCammon, J. A., & Karplus, M. (1980) *Annu. Rev. Phys. Chem. 31*, 29–45.
McCammon, J. A., Gelin, B. R., & Karplus, M. (1977) *Nature (London) 267*, 585–590.
McCammon, J. A., Wolynes, P. G., & Karplus, M. (1979) *Biochemistry 18*, 927–942.
Northrup, S. H., Pear, M. R., McCammon, J. A., Karplus, M., & Takano, T. (1980) *Nature (London) 287*, 659–660.
Northrup, S. H., Pear, M. R., Morgan, J. D., McCammon, J. A., & Karplus, M. (1981) *J. Mol. Biol. 153*, 1087–1109.
Parak, F., Frolov, E. N., Mössbauer, R. L., & Goldanskii, V. I. (1981) *J. Mol. Biol. 145*, 825–833.
Pauling, L., & Wilson, E. B., Jr. (1935) *Introduction to Quantum Mechanics*, McGraw-Hill, New York.
Peticolas, W. L. (1979) *Methods Enzymol. 61*, 425–458.
Richards, F. M. (1977) *Annu. Rev. Biophys. Bioeng. 6*, 151.
Snyder, G. H., Rowan, R., Karplus, S., & Sykes, B. D. (1975) *Biochemistry 14*, 3765–3777.
Stillinger, F. H., & Rahman, A. (1972) *J. Chem. Phys. 57*, 1281.
Tully, J. C. (1981) *Acc. Chem. Res. 14*, 188–194.
van Gunsteren, W. F., & Karplus, M. (1981) *Nature (London) 293*, 677–678.
van Gunsteren, W. F., & Karplus, M. (1982a) *Biochemistry 21*, 2259–2274.
van Gunsteren, W. F., & Karplus, M. (1982b) *Macromolecules* (in press).
Wagner, G., DeMarco, A., & Wüthrich, K. (1976) *Biophys. Struct. Mech. 2*, 139–158.
Wang, M. C., & Uhlenbeck, G. E. (1945) *Rev. Mod. Phys. 17*, 323–342.
Willis, B. T. M., & Pryor, A. W. (1975) *Thermal Vibrations in Crystallography*, Cambridge University Press, London.
Wilson, E. B., Jr., Decius, J. C., & Cross, P. C. (1955) *Molecular Vibrations*, McGraw-Hill, New York.
Zwanzig, R. (1965) *Annu. Rev. Phys. Chem. 16*, 67–102.

Analysis of Electrostatic Interactions and Their Relationship to Conformation and Stability of Bovine Pancreatic Trypsin Inhibitor†

Keith L. March, David G. Maskalick, Richard D. England, Stephen H. Friend,‡ and Frank R. N. Gurd*

ABSTRACT: The modified Tanford–Kirkwood electrostatic theory has been employed to evaluate pK values for all charge sites in the bovine pancreatic trypsin inhibitor (BPTI). ^{13}C NMR titration data were obtained for all titrating groups except arginine residues in BPTI at nearly constant ionic strength in 0.1 M NaCl, at 41 °C. The chemical shifts of 46 resonances were found to be sensitive to pH. The pK values of these titrating resonances compared well with those computed by the modified Tanford–Kirkwood electrostatic theory. A conformational change involving the NH_2- and COOH-terminal and nearby residues is shown to be partly electrostatically driven by the formation of a salt bridge between the α-amino and α-carboxyl groups at mid-pH values. The computed total electrostatic free energy of the molecule is found to be stabilizing at neutral pH despite the substantial net positive charge borne by the protein under such conditions.

Electrostatic interactions in biological macromolecules are widely recognized as crucial to structure–function relationships at every level. The Tanford–Kirkwood electrostatic theory as modified by Shire predicts in a detailed manner the pK values of individual charge sites within a protein (Shire et al., 1974a,b, 1975; Botelho et al., 1978; Matthew et al., 1979a,b) as well as the overall contribution of each site to the total electrostatic free energy of the molecule (Friend & Gurd, 1979a,b; Friend et al., 1980, 1981; Flanagan et al., 1981). Because of the exceptional stability of the bovine pancreatic trypsin inhibitor (BPTI) to extremes of pH and temperature (Vincent et al., 1971; Masson & Wüthrich, 1973; Harina et al., 1980; Wagner & Wüthrich, 1978) as well as its small size (Huber et al., 1970; Deisenhofer & Steigemann, 1975), it presents an opportunity to test the prediction of pK values for acidic and basic residues. The titrations of various amino acid residues in BPTI have been reported under many different conditions of ionic strength and temperature (Maurer et al., 1974; Snyder et al., 1975; Wagner & Wüthrich, 1975; Brown et al., 1976, 1978; Richarz

† From the Department of Chemistry and the Medical Sciences Program, Indiana University, Bloomington, Indiana 47405. *Received February 16, 1982.* This is the 129th paper in a series dealing with coordination complexes and catalytic properties of proteins and related substances. For the preceding paper, see Brown & Gurd (1981). This work was supported by U.S. Public Health Service Research Grants HL-05556 and HL-14680. K.L.M. and R.D.E. gratefully acknowledge support from Northwestern National Life Insurance Co. and American United Life, respectively, through the Insurance Medical Scientist Scholarship Fund.

‡ Present address: Department of Pediatrics, Children's Hospital of Philadelphia, Philadelphia, PA.

0006-2960/82/0421-5241$01.25/0

& Wüthrich, 1978), making comparisons with predictions of the electrostatic theory difficult. This report presents ^{13}C NMR titration data for all titrating groups except arginines in BPTI at nearly constant ionic strength in 0.1 M NaCl at 41 °C. This self-consistent set of titration data was compared with the pK values predicted by the electrostatic theory as well as those determined previously by ^{1}H and ^{13}C NMR (Snyder et al., 1975; Brown et al., 1976, 1978; Richarz & Wüthrich, 1978). The ^{13}C NMR data are used in conjunction with the theory to substantiate further the existence in solution of a salt bridge between the α-carboxyl and the α-amino groups in the mid-pH range and to characterize the conformational change associated with its formation (Brown et al., 1978). This salt bridge is not present in the crystal structure determined at high pH (Deisenhofer & Steigemann, 1975). It contributes to the computed net electrostatic stabilization of the molecule found even at neutral pH where a substantial net positive charge is present.

Methods

Electrostatic Proton-Binding and Free-Energy Calculations. The procedure for the iterative electrostatic interaction calculation has been described elsewhere (Matthew et al., 1979a, 1981, 1982; Friend & Gurd, 1979a,b; Flanagan et al., 1981). The electrostatic free energy of interaction, between a pair of positive unit charges, W_{ij}, is a function of several model parameters (Tanford & Kirkwood, 1957; Friend et al., 1980). These include internal and external dielectric constants, ionic strength, and the distance of closest approach of a counterion to the protein surface.

So that the irregular protein solvent interface can be accounted for, the energy of interaction between pairs of charges, W_{ij}, is modulated by the fractional accessibility of the charged atoms to the solvent:

$$W'_{ij} = W_{ij}(1 - \overline{SA}_{ij}) \quad (1)$$

where $\overline{SA}_{ij}$ is the average static accessibility of the ith and jth groups (Lee & Richards, 1971; Matthew et al., 1978a). This formalism leads to substantially the same results in the iterative procedure as that starting from the form $W'_{ij} = W_{ij}(1 - SA_j)$ that was previously adopted. The newer formalism avoids the asymmetry, and the calculations converge more rapidly (Matthew et al., 1982; Matthew & Richards, 1982). The intrinsic equilibrium constant in the absence of effects from other charged sites, $(pK_{int})_i$, is modulated by the extent of electrostatic interactions of site i with other charged sites j:

$$pK_i = (pK_{int})_i - \frac{1}{2.303kT}\sum_{j\neq i}^{n} W'_{ij}Z_j = (pK_{int})_i + \sum_{j\neq i}^{n}\Delta pK_{ij} \quad (2)$$

where Z_j is the fractional charge on site j. A consistent set of pK_i values is computed at each pH and ionic strength by using an iterative procedure (Shire et al., 1974a,b; Matthew et al., 1978b; Botelho et al., 1978). The parameter $pK_{1/2}$ is defined as the pH at which a particular residue is half-titrated and is the computed value used to compare with experimental pK values.

The overall electrostatic free energy calculated for a protein summed over its n charged sites is given by

$$\Delta G_{el} = \tfrac{1}{2}\sum_{i=1}^{n}\sum_{j\neq i}^{n} W'_{ij}Z_iZ_j = \frac{2.303kT}{2}\sum_{i=1}^{n}\sum_{j\neq i}^{n}\Delta pK_{ij}Z_i \quad (3)$$

This form differs from that used previously in which separate $1 - SA_j$ terms were used for each site instead of the average as employed here. The effect of the alteration in definition is not large in most cases and renders the argument consistent.[1]

BPTI Parameters for Electrostatic Calculations. The average radius of the equivalent sphere was taken as 11.4 Å from the crystallographic molecular volume (Huber et al., 1970; Deisenhofer & Steigemann, 1975), and the ion-exclusion parameter was taken as 13.4 Å. The atomic coordinates refined to 1.5-Å resolution (Deisenhofer & Steigemann, 1975) were obtained from the Protein Data Bank at the Brookhaven National Laboratory (Bernstein et al., 1977). The pK_{int} values for each group were those used previously (Botelho et al., 1978; Matthew et al., 1979a) and that for the α-amino group was taken as 7.60 as in hexaglycine (Cohn & Edsall, 1943).

Tyr-23 is titratable only in conjunction with a time-dependent irreversible denaturation of the protein (Scholtan & Rosenkranz, 1966; Sherman & Kassell, 1968), and its iodination (Sherman & Kassell, 1968) and nitration (Meloun et al., 1968) are prohibited in the native conformation. It has thus been considered as a "masked" residue and is omitted from the set of charge-bearing sites used in the calculations. Although Tyr-35 is not reactive to nitration conditions (Meloun et al., 1968), it is susceptible to diiodination, demonstrates reversible titration (Scholtan & Rosenkranz, 1966; Sherman & Kassell, 1968), and is included as a titrating site along with Tyr-21 and Tyr-10.[2]

For functional groups with delocalized charge structure such as guanidinium or carboxylate moieties, the charge was assigned to the atom of highest SA, as suggested by Matthew et al. (1978b), unless dictated otherwise by H-bonding or salt-bridge patterns.

A progression of plausible modified conformations for electrostatic comparison with native BPTI was determined, utilizing motion of only the COOH terminus as it was brought into apposition with the NH_2 terminus. Coordinates were computed for a series of 13 structures representing stages in the adjustment of the four concomitant bond rotations involved, with the contact limit between the α-amino nitrogen, N_1, and the nearest α-carboxyl oxygen, O_{58}, first attained in structure **10**. The actual conformational change is likely only analogous to that defined with this series of intermediate structures, especially in light of the difficulty in localizing the COOH terminus crystallographically (Deisenhofer & Steigemann, 1975). Further description of the modeling procedure for this structural transition is provided in the supplementary material (see paragraph at end of paper regarding supplementary material).

Theory of Titration with Associated Conformational Equilibria. The model used to analyze and interpret experimental pK values in terms of a conformational transition controlled by electrostatic and nonelectrostatic factors was

[1] The use of the $1 - \overline{SA}_{ij}$ term in the calculation of pK_i yields values which differ somewhat from those obtained by the earlier method. The differences range from 0.00 to 0.16 pK unit and average 0.05 pK unit. The use of the $1 - \overline{SA}_{ij}$ term in the calculation of $\Delta G_{i,el}$ results in values of greater magnitude than those obtained by the earlier method. The increase in $\Delta G_{i,el}$ is much more pronounced for exposed sites than for buried sites. The effect upon the overall ΔG_{el} is limited because the relative contribution to the overall ΔG_{el} by exposed sites is much less than the relative contribution by buried sites. Thus, with the $1 - \overline{SA}_{ij}$ term, $\Delta G_{el} = -1.28$ kcal/mol, whereas with the $(1 - SA_i)(1 - SA_j)$ term, as in earlier calculations, $\Delta G_{el} = -0.89$ kcal/mol, at pH 6.0, and $I = 0.10$ M.

[2] The Tyr-35 hydroxyl is hydrogen bonded to the Cys-38 amide nitrogen (Deisenhofer & Steigemann, 1975), and its pK_{int} is accordingly taken as 10.50 (Table V). As previously, it is assumed that hydrogen bonding of charge sites shifts their pK_{int} values by +0.5 or −0.5 unit, according to their proton- or electron-donating role (Matthew et al., 1979a). For interactions involving two charge sites in a close ion pair, however, the pK_{int} values are considered to be normal in order to avoid double consideration of their polar nature.

Scheme I: Conformational Equilibria of the BPTI Termini

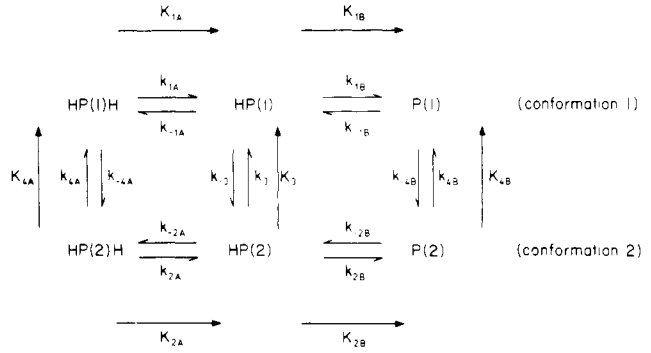

closely analogous to that employed by Russu et al. (1980) for the β-146 region of hemoglobin. The pertinent conformational and protonation equilibria may be represented as in Scheme I, where HP(1)H, HP(1), and P(1) are three protonation states of conformation 1 in which the α-amino group is held near the α-carboxyl group, such that they can form a salt bridge, and HP(2)H, HP(2), and P(2) represent conformation 2 in which both groups are relatively free, with their pK values accordingly closer to neutrality. The two proton sites represent these two groups, respectively. The symbols k and K, respectively, represent rate constants and corresponding equilibrium constants. Subscript A specifies the low pH (α-carboxyl related) values and subscript B the analogous high pH (α-amino related) parameters.

K_3 in Scheme I characterizes the interconversion between conformations 1 and 2, when both termini are charged. It may be written as K_{3A} when it is calculated with reference to the protonation equilibrium of the α-carboxyl group and K_{3B} with reference to the deprotonation equilibrium of the α-amino group. These values should coincide if the HP(2)H and P(2) forms of conformation 2 are equivalent.

Any carbon in the Arg-1 or Ala-58 residue may in principle exhibit a ^{13}C NMR spectrum of a form dependent upon the magnitude of the rate constants k_i and k_{-i} (i = 1–4) relative to each other and to the NMR time scale. In a system for which both the exchange rates of protons and the exchange rates between the two conformations (i.e., k_i^{-1} and k_{-i}^{-1}) are fast relative to the NMR time scale, only one resonance per nucleus should be observed in the ^{13}C NMR spectrum. This appears to be the case for the terminal titrations observed in this study. Following the derivation of Russu et al. (1980), it may be shown that when conformation effects on chemical shifts are small compared to the protonation effects (Markley & Finkenstadt, 1975), the observed equilibrium constant K_{obsd} for both the α-amino and α-carboxyl titrations is given by

$$K_{obsd,B} = \frac{K_{2B} + K_{1B}K_{3B}}{1 + K_{3B}}$$
$$K_{obsd,A} = \frac{1 + K_{3A}}{1/K_{2A} + K_{3A}/K_{1A}} \quad (4)$$

In this limit the titration curve will be of the simple Henderson–Hasselbalch type.

Sample Preparation. BPTI from Novo Industries, Denmark, was subjected to repeated ultrafiltration and dilution with distilled deionized H_2O to remove any salts followed by addition of NaCl to a total concentration of 0.10 M. The protein solution was then concentrated to about 22 mM. The sample volume was restricted to between 4 and 5 mL in a 15-mm sample tube.

^{13}C NMR Collection Parameters. Natural abundance ^{13}C NMR spectra were obtained with a 63.4 kG (67.9 MHz) spectrometer utilizing a Bruker HX270 superconducting solenoid and 15-mm ^{13}C NMR probe. For ^{13}C excitation, 56° pulses of 12.1-μs duration were used for optimum signal from carbons with spin–lattice relaxation times near 1 s (Ernst & Anderson, 1966). The radio-frequency pulse was set 38.875 ppm downfield from the ^{13}C resonance of external neat ethylene glycol. Each spectrum utilized quadrature phase detection and represents 16 384 accumulations with a recycle time of 0.59 s (161 min total time). Time-domain data were accumulated in 8192 addresses with a spectral width of 13 888 Hz. Full proton decoupling with square wave modulation centered 1.4 ppm downfield from Me_4Si effectively decoupled methyl carbon resonances between 0 and 25 ppm and the carbonyl region between 166 and 186 ppm as well as providing adequate conditions for observing narrow nonprotonated aromatic carbon resonances.

^{13}C NMR Titration. The pH was adjusted with 5–40 μL of reagent grade 1 N NaOH or 1 N HCl and was measured with a Radiometer PHM4c meter and Ingold AgCl electrode at 41 °C, the sample temperature in the ^{13}C NMR probe ±1 °C. As acid or base was added, the titration was done in two parts in order to limit the effect of changing ionic strength. Twenty-six spectra were collected between pH 7.49 and pH 1.78 by addition of HCl, and 18 spectra were collected between pH 6.92 and pH 10.41 by addition of NaOH. At the acid and base limits of the titration, the ionic strength was calculated to be 0.15 and 0.13 M, respectively.

The spectra were processed by a convolution difference technique (Campbell et al., 1973) that involved multiplying the free induction decay by $(e^{-t/0.313} - 0.775e^{-t/0.104})$. This technique increased the resolution of lines having widths between 5 Hz and 12 Hz without significantly decreasing the signal to noise ratio.

Chemical shifts were measured relative to the downfield isoleucine resonance which was taken to be 12.285 ppm from Me_4Si when measured relative to internal dioxane. The chemical shift of this resonance had been found to be insensitive to pH. The ppm vs. pH data were analyzed by fitting the data to the Henderson–Hasselbalch equation by using unweighted nonlinear least-squares regression according to the Gauss–Newton method (Sampson, 1970). The pK values determined by ^{13}C NMR at 41 °C were subsequently converted to their effective values at 25 °C for comparison with the electrostatic calculations by use of the van't Hoff equation and the apparent heats of ionization, ΔH, for each particular functional group (Tables I–IV) assuming that ΔH is independent of temperature between 0 and 41 °C (Cohn & Edsall, 1943).

Results and Discussion

NMR Spectra. The entire ^{13}C NMR spectrum shown in Figure 1 has been divided into four parts based on the chemical shifts of different carbon types referred to those represented in the pentapeptide Gly-Gly-X-Gly-Gly where X is the amino acid of interest (Gurd et al., 1972; Keim et al., 1973a,b, 1974; P. Keim, R. A. Vigna, and F. R. N. Gurd, unpublished results). From the spectrum in Figure 1B without NOE enhancement (Kuhlman & Grant, 1971), these four regions were integrated and normalized relative to the α-carbon region. Figure 1 shows that each spectral region holds a normalized intensity, shown in part A, equivalent to that expected on the basis of the amino acid composition (Kassell & Laskowski, 1965) and the pentapeptide chemical shifts, shown in part C. The carbonyl and aromatic regions exhibit integrals slightly less than expected due to saturation of the nonprotonated carbon resonances (Norton et al., 1977). The separate regions

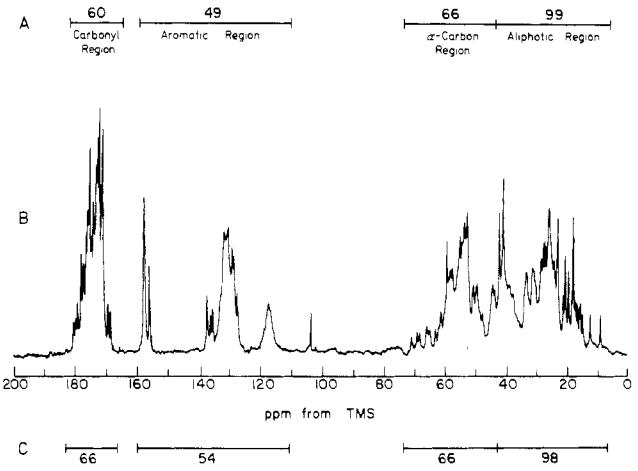

FIGURE 1: Entire 67.9-MHz natural abundance ^{13}C NMR spectrum of BPTI without NOE enhancement. (A) The number of carbons in each spectral region obtained by integrating and normalizing relative to the α-carbon region. (B) Normal Fourier transform spectra of 28 mM BPTI representing 8192 accumulations with gated proton decoupling, 5-s recycle time, and 90° ^{13}C excitation pulse of 19.5 μs, spectral width 16 129 Hz; all other parameters the same as outlined under Methods. (C) The number of carbons expected to contribute resonances in each region based on the amino acid composition of BPTI and the chemical shifts of carbons in the model pentapeptides, Gly-Gly-X-Gly-Gly where X is the amino acid of interest (Keim et al., 1973a,b, 1974; P. Keim, R. A. Vigna, and F. R. N. Gurd, unpublished results).

of the spectrum shown in Figure 1 are presented in Figures 2–5 for which the data collection and processing are described under Methods.

Figures 2–5 are constructed to show, for each region of the spectrum, (A) the characteristic chemical shifts of resonances observed in the pentapeptides including those observed at pH extremes, connected by horizontal lines, (B) the pH dependence of the pH-sensitive protein resonances, and (C) the observed resonances in the protein at pH values near 7 with pH-sensitive resonances identified by numerals corresponding to the titrations in (B). For example, in the aliphatic region shown in Figure 2, on the basis of the amino acid composition, seven single carbon resonances should titrate at acid pH values between limits approximately indicated in Figure 2A, as was found experimentally (Figure 2B). Each titrating resonance can be assigned as to carbon type by comparison with three characteristics of the pentapeptide model compounds: (i) the chemical shifts of the protonated and deprotonated states, (ii) the overall chemical shift differences between the protonated and deprotonated states, hereafter called the titration shift, and (iii) the pK values. These characteristics of the pentapeptides are available in an expanded version of Tables I–IV appearing in the supplementary material listed as Tables Ia–IVa. The titrating protein resonances can further be tentatively correlated with specific amino acid residues in the BPTI sequence by rank order comparisons of the observed pK to the p$K_{1/2}$ computed according to the modified Tanford–Kirkwood electrostatic theory, also included in Tables I–IV. The tentative assignments along with the relevant data for resonances 1–7, seen in Figure 2, are shown in Tables I and II.

The lysine C^{δ} and Arg-1 C^{β} and C^{γ} resonances exhibit detectable titrations (Figure 2) while those peaks believed to represent lysine C^{δ}, C^{γ}, and C^{ϵ} carbons and the Arg-1 C^{δ} carbon appear to be relatively insensitive to pH within resolution limitations. Only one lysine C^{γ} resonance is resolved well enough to detect its titration shift, which is characteristically so small that the pK cannot be estimated with sufficient accuracy for correlation to a specific corresponding lysine C^{δ}

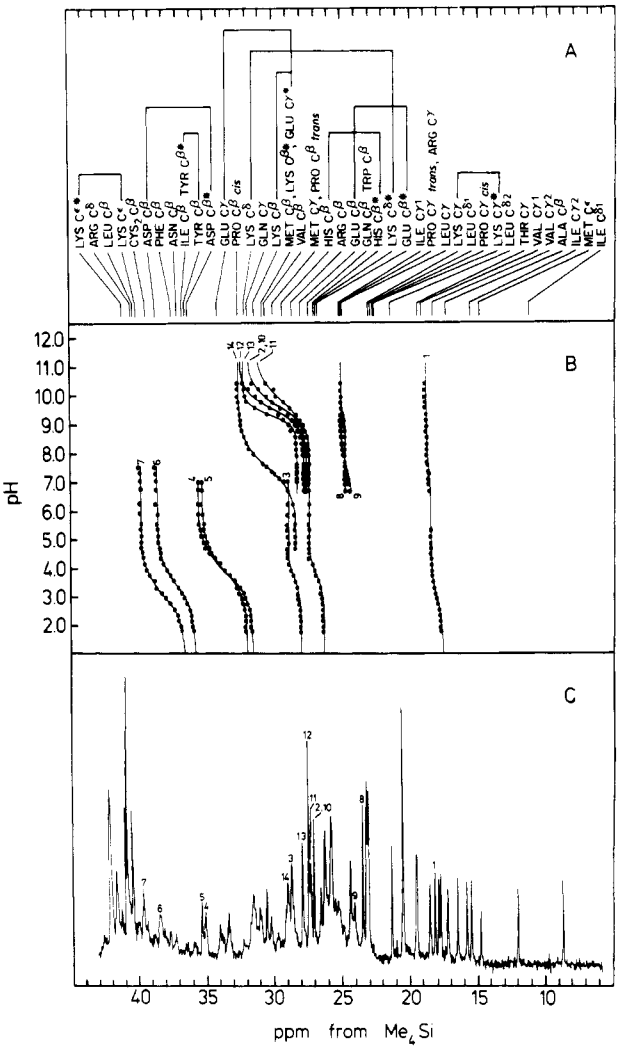

FIGURE 2: Aliphatic region of the 67.9-MHz natural abundance ^{13}C NMR spectrum of BPTI. (A) The chemical shifts and titration shifts of carbons contributing resonances to the aliphatic region, as observed in pentapeptides of the form Gly-Gly-X-Gly-Gly where X is the amino acid of interest (Keim et al., 1973a,b, 1974; P. Keim, R. A. Vigna, and F. R. N. Gurd, unpublished results). Asterisk indicates chemical shift corresponding to the protonated state of the side chain. (B) Plot of the chemical shifts of all the individual titrating resonances observed in the aliphatic region vs. the pH at which each spectrum was accumulated. For dually labeled titration curves the numbers represent the low- and high-pH titrations, respectively. (C) The aliphatic region of the ^{13}C NMR spectrum of BPTI, pH 6.92, 6–43 ppm from Me_4Si, obtained as described under Methods.

resonance. The Arg-1 and lysine assignments appear in Tables II and III, respectively.

In the carbonyl region (Figure 3), according to the amino acid composition there should be a maximum of nine titrating resonances at acid pH values, all of which should move downfield upon deprotonation according to the pentapeptide titration data (Figure 3A). Figure 3B indicates that 15 out of approximately 53 resonances have pH-dependent chemical shifts. Peaks 19, 20, 23, 35, 26, 27, and 29 were correlated with particular carbons in the BPTI sequence as shown in Tables I and II.

Since pK values and C^{α} resonance titration shifts of lysines and tyrosines are similar, and because only small pK nonequivalences are expected between the individual lysines and individual tyrosines, the assignment of each carbonyl peak titrating in the alkaline range to an amino acid in the sequence could not be made with reasonable certainty. Nevertheless, 8 of the 11 alkaline carbonyl titration shifts appeared to titrate

Table I: Acid pK Values and Assignments

amino acid assignment for pK_{obsd}	carbon atom	peak	obsd δ_A	obsd δ_B	lit.[a] pK (error)	obsd[b] pK_{eff} (SD)	computed $pK_{1/2}$	amino acid residue for $pK_{1/2}$
Glu-7, Glu-49	β	3	27.77	28.82	NR	3.63 (0.07)	4.23	Glu-7
	γ	4	31.43	35.37	3.7 (0.2)	3.95 (0.02)		
	δ	27	178.05	181.58	3.6 (0.2)	3.89 (0.04)	*4.05*	
	o	25	176.64	177.41	NR	3.92 (0.09)		
	β	2	26.10	27.24	NR	3.74 (0.07)	4.43	Glu-49
	γ	5	31.85	35.10	3.8 (0.2)	3.99 (0.02)	*4.38*	
	δ	28	177.94	182.26	3.7 (0.2)	4.01 (0.02)		
Asp-3, Asp-50	β	6	35.68	38.43	3.4 (0.2)	3.55 (0.02)	3.93	Asp-3
	γ	19	174.54	177.81	3.4 (0.2)	3.58 (0.02)	*3.87*	
	o	26	176.87	178.11	NR	3.52 (0.06)		
	β	7	36.44	39.63	3.0 (0.2)	3.20 (0.02)	2.89	Asp-50
	γ	20	173.70	177.01	3.1 (0.2)	3.17 (0.02)	*2.58*	
	o	23	174.95	176.09	NR	3.24 (0.04)		

[a] Literature values taken from Richarz & Wüthrich (1978) for the protein pK values. [b] $pK_{eff} = pK(25\ °C) = pK_{obsd}(41\ °C) + C$ where $C = 0.04$ for Glu and $C = 0.08$ for Asp. NR = not reported. Values in italics were calculated at $I = 0.01$ M; others were calculated at 0.10 M which corresponds with the experimental conditions used in this study.

Table II: Cotitrations of NH_2 and COOH Terminal

amino acid assignment for pK_{obsd}	carbon atom	peak	obsd δ_A	obsd δ_B	lit.[a] pK (error)	obsd[b] pK_{eff} (SD)	computed $pK_{1/2}$	amino acid residue for $pK_{1/2}$
Ala-58[c]	β	1[e]	17.47	18.30	2.8 (0.2)	3.02 (0.08)		
	α	38[f]	50.05	52.54	2.7 (0.2)	3.07 (0.02)	3.49[h]	Ala-58
	o	29[g]	178.08	181.30	3.0 (0.2)	3.20 (0.02)		
Arg-1[d]	o	15	168.69	169.01	3.0 (0.1)	3.47 (0.13)	*i*	Arg-1
Arg-1[d]	β	14	28.19	32.40	NR[j]	7.93 (0.01)		
	γ	9	24.06	24.91	NR	7.79 (0.08)	7.56[h]	Arg-1
	o	15	169.06	175.88	~8.0	7.94 (0.02)		
Ala-58[c]	β	1	18.44	18.74	8.0 (0.3)	8.59 (0.28)	*i*	Ala-58
	o	29	181.36	180.76	8.2 (0.7)	7.69 (0.14)		

[a] Literature values taken from Brown et al. (1978). [b] $pK_{eff} = pK(25\ °C) = pK_{obsd}(41\ °C) + C$ where $C = -0.02$ for the COOH terminal and $C = +0.42$ for the NH_2 terminal. [c] The chemical shifts of alanine C^o, C^α, and C^β in the pentapeptide Gly-Gly-Ala-Gly-Gly are 176.7, 51.3, and 17.9 ppm, respectively. [d] The chemical shifts of arginine C^o, C^β, and C^γ in the pentapeptide Gly-Gly-Arg-Gly-Gly are 175.35, 29.2, and 25.7, respectively. [e] Peak 1 is assigned to Ala-58 C^β since it titrates in the methyl carbon region where no other titrations should or do occur. [f] Peak 38 is assigned to Ala-58 C^α and is distinguished from an aspartate C^α because its titration shift compares more favorably with that for the C^α of Gly-5 in the pentapeptide $(Gly)_5$. [g] Peak 29 cannot be distinguished from an aspartate C^γ except that its δ_A is closer to the chemical shift of Ala C^o in the pentapeptide than peaks 19 and 20. Also both peaks 19 and 20 have δ_A values closer to the δ_A of Asp C^γ in the pentapeptide than peak 29. The titration of peak 29 at high pH along with the titration of peak 1 already assigned to Ala-58 C^β confirms the assignment of peak 29 to Ala-58 C^o. [h] Computed with the conformational change ignored. [i] Should not titrate in this pH range. [j] NR = not reported.

Table III: Lysine pK Values and Assignments

amino acid assignment for pK_{obsd}	carbon atom	peak	δ_A	δ_B	lit.[a] pK	obsd[b] pK_{eff} (SD)	computed $pK_{1/2}$	amino acid residue for $pK_{1/2}$
Lys-46, -26, -15	δ	13	27.90	32.96		9.87 (0.10)	10.35, *10.35*[e]	Lys-46
	δ	12	27.50	33.04	10.6[c]	10.10 (0.05)	10.43, *10.42*	Lys-26
	δ	10	27.12	32.43		10.19 (0.05)	10.43, *10.43*	Lys-15
Lys-41	δ	11	27.52	32.90[d]	10.8	10.6 (0.03)	10.70, *10.78*	Lys-41
Lys ?	γ	8	24.56	25.10		10.0 (0.1)		
Lys-15, -26, -41, -46	o	34	173.87	174.36		9.8 (0.1)		
	o	32	172.03	172.33		10.1 (0.1)		
	o	37	177.86	178.24		10.2 (0.1)		
	o	36	176.12	176.45		10.2 (0.2)		

[a] Literature values taken from Brown et al. (1976). [b] $pK_{eff} = pK(25\ °C) = pK_{obsd}(41\ °C) + C$ where $C = 0.42$. [c] Represents the pK for a single peak representing three unresolved proton resonances. [d] Fixed base limit for pK calculation since incompletely titrated. [e] Values in italics were calculated at $I = 0.01$ M: others were calculated at 0.10 M which corresponds with the experimental conditions used in this study.

with the four lysines and the four tyrosines; see Tables III and IV. The Arg-1 C^o peak assignment and titration data are found in Table II.

Analysis of titrations in the C^α region, other than the low pH titration of Ala-58 C^α (Figure 4B), was not pursued since the same pK values could be obtained more accurately from other spectral regions. In Figure 4C the 13 resolved downfield peaks, representing 14 single carbon resonances, can be tentatively assigned by the pentapeptide values summarized in Figure 4A to arise from three threonine C^β, one serine C^β, three threonine C^α, two isoleucine C^α, one valine C^α, and four proline C^α. Table II shows the pK and other relevant data for Ala-58 C^α.

Figure 5B shows the pH dependence of the four tyrosine C^γ resonances, peaks 39–42, and the four tyrosine C^ζ resonances, peaks 51–54. The four phenylalanine C^γ resonances,

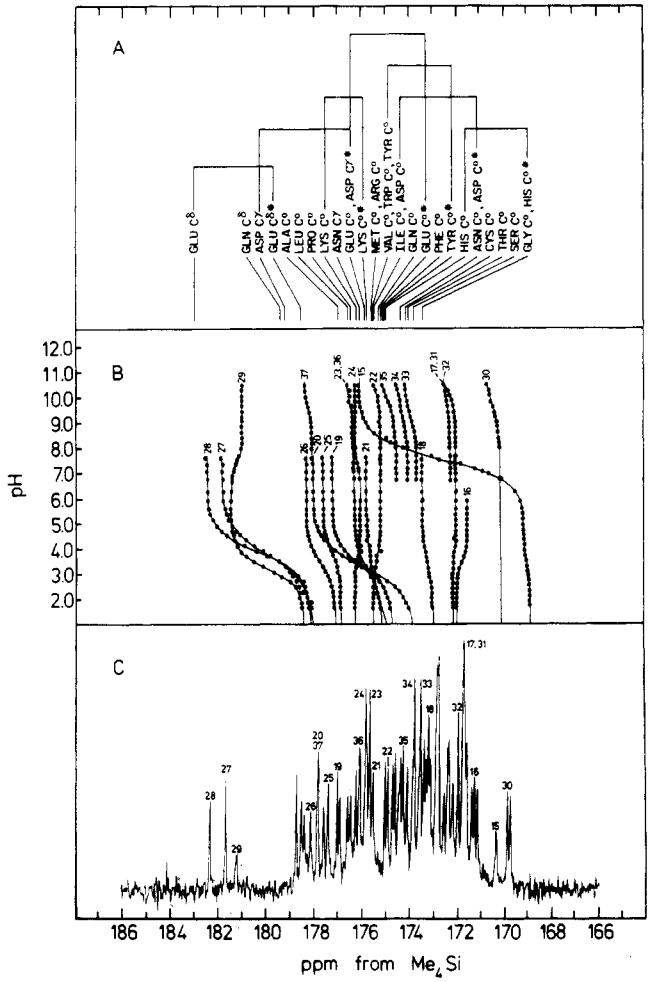

FIGURE 3: Carbonyl region of the 67.9-MHz natural abundance ^{13}C NMR spectrum of BPTI. (A) The chemical shifts and titration shifts of carbonyl and carboxyl carbons in the series of pentapeptide model compounds Gly-Gly-X-Gly-Gly (Keim et al., 1973a,b, 1974; P. Keim, R. A. Vigna, and F. R. N. Gurd, unpublished results). Asterisk indicates chemical shift corresponding to the protonated state of the side chain. (B) Plot of the chemical shifts of all the individual titrating resonances observed in the carbonyl region against pH. For dually labeled titration curves the numbers represent the low- and high-pH titrations, respectively. (C) The carbonyl region of the ^{13}C NMR spectrum of BPTI, pH 6.92, 166–186 ppm from Me_4Si, obtained as described under Methods.

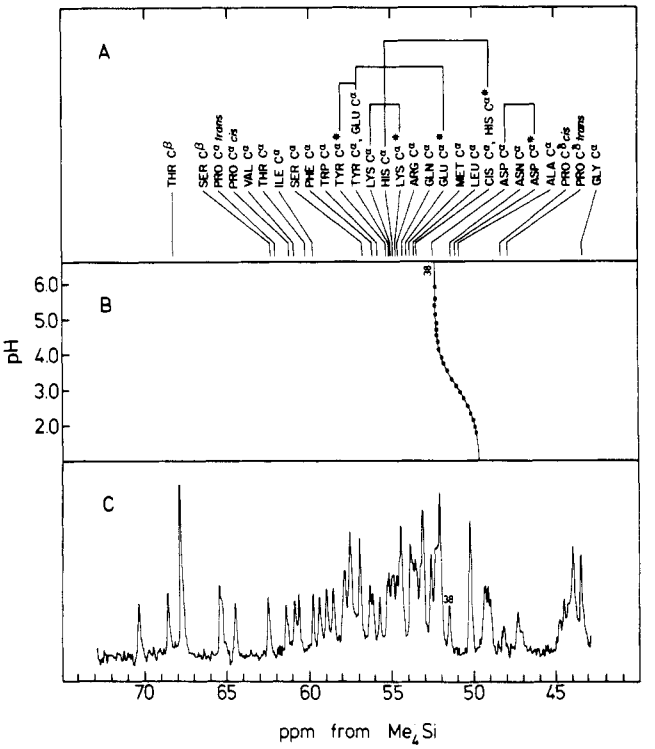

FIGURE 4: α-carbon region of the 67.9-MHz natural abundance ^{13}C NMR spectrum of BPTI. (A) The chemical shifts and titration shifts of carbons contributing resonances to the α-carbon region from the series of pentapeptide model compounds Gly-Gly-X-Gly-Gly (Keim et al., 1973a,b, 1974; P. Keim. R. A. Vigna, and F. R. N. Gurd, unpublished results). Asterisk indicates chemical shift corresponding to the protonated state of the side chain. (B) The dependence on pH of the chemical shift of peak 38 assigned to alanine-58 C^{α}. (C) The α-carbon region of the ^{13}C NMR spectrum of BPTI, pH 3.20, 43–73 ppm, obtained as described under Methods except with the proton decoupling frequency centered 5 ppm downfield from Me_4Si. The large peak at 67.8 ppm is due to dioxane which was added as an internal reference. In a spectrum obtained without dioxane present it was found that a sharp protein resonance also appeared in this position.

peaks 43–46, and the six arginine C^{ζ} resonance, peaks 47–50, appear to be insensitive to pH <10.41. The modulated off-resonance decoupling used efficiently broadens the mono-protonated methine aromatic carbon resonances, leaving the narrow nonprotonated carbon resonances well-defined and thus simplifying the aromatic region. This method has been described more fully elsewhere (Oldfield et al., 1975; Wenkert et al., 1969). The tyrosine peaks were specifically assigned, Table IV, by comparison to the rank order of pK values determined by ^1H NMR (Snyder et al., 1975), where the tyrosines were assigned on the basis of nitration and iodination experiments. The ^{13}C NMR titrations of the C^{ζ} resonances obtained here differ significantly from those reported previously at much lower resolution and signal/noise ratio (Maurer et al., 1974).

Discrepancies between ^{13}C NMR and ^1H NMR pK Values. The lysine and tyrosine pK values determined here by ^{13}C NMR are significantly lower than those determined by ^1H NMR. The lysine pK values obtained by ^1H NMR were determined at unreported temperature and ionic strength and 10 mM protein in D_2O (Brown et al., 1976), whereas the tyrosine pK values obtained by ^1H NMR were determined at 28 °C in a combination buffer composed of 0.1 M KCl, 15 mM Tris, 15 mM aspartate, 15 mM phosphate in D_2O, and 2.5 mM protein concentration (Snyder et al., 1975). Tyrosine pK values determined by Wagner & Wüthrich (1975) by using ^1H NMR at 22 °C, unreported ionic strength, and 10 mM protein in D_2O also differed from those values reported by Snyder et al. (1975). Possible sources of the discrepancies are differences in ionic environments, solvent hydrogen-isotope, protein concentration, and temperature.

Cotitrations of the Termini. The double-titration shifts of peaks 1, 29, and 15 (Figures 2 and 3; Table II) confirm the report that the carbons associated with the two termini each experience the titration of the other partner (Brown et al., 1978). It has been postulated that the terminal residues form a salt bridge in the mid-pH range where both retain charges. This would explain the lowered α-carboxyl and elevated α-amino pK values as well as the cotitration of each peak as the pH nears the pK of the other terminus, as shown in Table II. The postulate of the salt bridge formation requires an altered conformation for the mid-pH solution structure relative to the high pH crystal structure.

Chemical Shift Changes of Resonances from Nonionizable Amino Acids. Peaks 16, 17, 18, 21, 22, and 24 show pH-sensitive chemical shifts (Figure 3). Because all titrations of ionizable groups in the carbonyl region except for one gluta-

Table IV: Tyrosine pK Values and Assignments

amino acid assignments for pK_{obsd}	carbon atom	peak	δ_A	δ_B	lit.[a] pK (SD)	obsd[b] pK_{eff} (SD)	computed $pK_{1/2}$	amino acid residue for $pK_{1/2}$
Tyr-10	γ	39	128.30	122.52	10.4 (0.2)	9.45 (0.02)	9.95[f]	Tyr-10
	ζ	54	156.20	165.62		9.48 (0.02)	*9.87*	
Tyr-21	γ	41	130.07	124.68	11.0 (0.2)	9.98 (0.03)	10.05	Tyr-21
	ζ	53	156.34	164.28		9.90 (0.03)	*10.04*	
Tyr-35	γ	40	127.33	119.99	11.1 (0.2)	10.6 (0.04)	10.22	Tyr-35
	ζ	52	157.67	166.90		10.6 (0.03)	*10.05*	
Tyr-23	γ	42	128.94	124.70	11.7 (0.2)	10.9 (0.06)	*d*	Tyr-23
	ζ	51	156.20	165.50		11.1 (0.03)		
Tyr-10, -21, -23, -35	o	33	173.45	173.98		9.4 (0.1)		
	o	30	169.96	170.58		9.7 (0.1)		
	o	35	174.33	174.94		10.0 (0.1)		
	o	31	171.82	*e*		>10.3[c]		

[a] Literature values taken from Snyder et al. (1975). [b] $pK_{eff} = pK(28\ ^\circ C) = pK_{obsd}(41\ ^\circ C) + C$ where $C = 0.19$. [c] Shift too small for accurate calculation of pK. [d] Tyr-23 should not reversibly titrate, as indicated under Methods. If this group is considered as unmasked, its $pK_{1/2}$ values are computed to be 10.21 and 10.18 at $I = 0.10$ and 0.01, respectively. The unlikely presence of this extra charge in the native structure is calculated to perturb $pK_{1/2}$ values by 0.04 unit at most. [e] Not completely titrated and cannot be calculated. [f] Values in italics were calculated at $I = 0.01$ M; others were calculated at 0.10 M which corresponds with the experimental conditions used in this study.

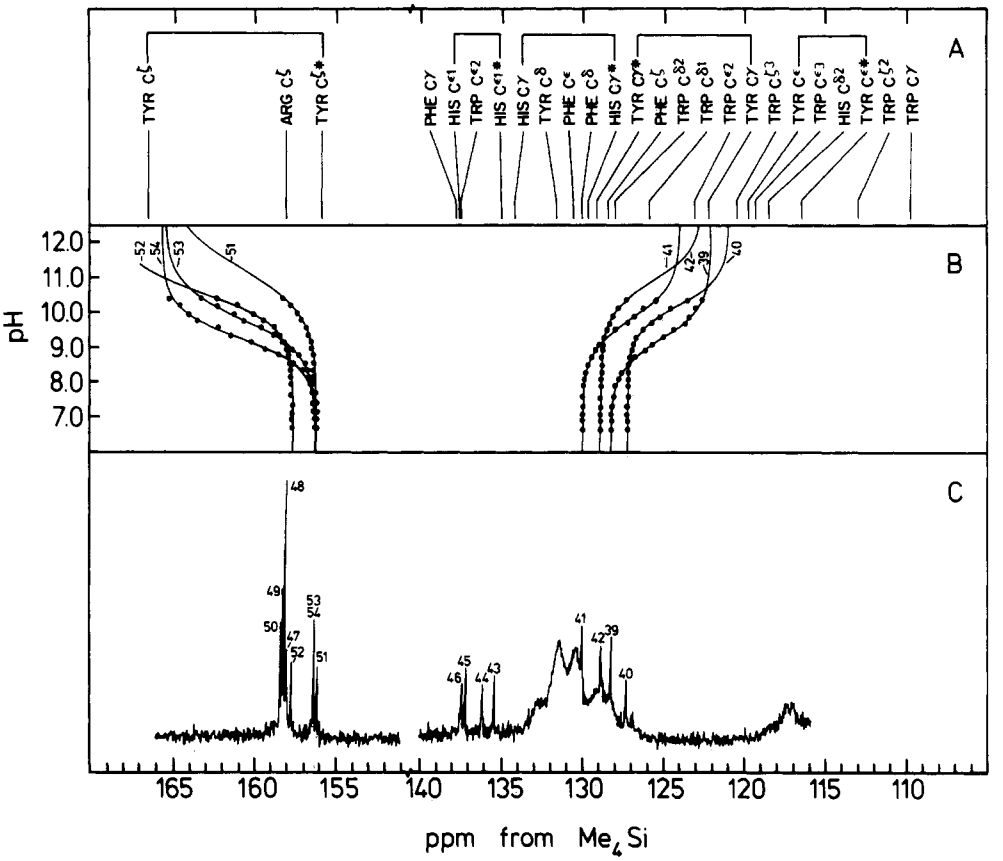

FIGURE 5: Aromatic region of the 67.9-MHz natural abundance ^{13}C NMR spectrum of BPTI. (A) The chemical shifts and titration shifts of carbons contributing resonances to the aromatic region from the series of pentapeptide model compounds Gly-Gly-X-Gly-Gly (P. Keim, R. A. Vigna, and F. R. N. Gurd, unpublished results). Asterisk indicates chemical shift corresponding to the protonated state of the side chain. (B) Plot of the chemical shifts of the individual titrating nonprotonated carbon resonances in the aromatic region against pH. (C) The aromatic region of the ^{13}C NMR spectrum of BPTI, 116–166 ppm from Me_4Si, pH 6.92, obtained as described under Methods.

mate C$^\alpha$ have been accounted for, five of these peaks must result from carbons of nonionizable residues.

In the pentapeptide model compounds the backbone carbonyl carbons adjacent to the NH_2- and COOH-terminal residues experience either upfield or downfield titration shifts of between 0.25 ppm and 1.0 ppm. Thus, one of the extra carbonyl titrations in the acid range, probably peak 16, may represent Gly-57 C$^\alpha$. One of the two extra downfield titrations, peak 18 or 21, may result from a glutamate C$^\alpha$. The four remaining unexplained carbonyl titration shifts in the acid range are probably due to conformational changes of the peptide backbone.

If the crystal conformation determined at high pH is similar to both the acid and base solution conformations but the mid-pH range conformation is different in that the two termini have approached each other to form a salt bridge, then any resonances that sense this conformational change would have similar chemical shifts at low and high pH values and experience a double titration reflected about the mid-pH range. Peaks 22 and 24 exhibit this behavior. Previously reported

Table V: Parameters of Titrating Groups in BPTI

group	residue no.	atom	pK_{int}	1 − SA
C terminal	58	O	3.60	0.05
Asp	50	OD1	4.00	0.65
	3	OD2	4.00	0.05
Glu	7	OE1	4.50	0.45
	49	OE1	4.50	0.05
N terminal	1	N	7.60	0.16
Tyr	21	OH	10.00	0.25
	10	OH	10.00	0.40
	35	OH	10.50	0.85
Lys	46	NZ	10.40	0.20
	26	NZ		0.05
	15	NZ		0.15
	41	NZ		0.21
Arg	1	NT2	12.00	0.30
	17	NT1		0.10
	42	NT1		0.10
	53	NT1		0.70
	39	NT1		0.05
	20	NT1		0.50

evidence for the interterminal conformational change included chemical shift differences between the native BPTI and the form in which the α-amino group was altered by transamination (Brown et al., 1978). In that case changes were observed in the chemical shifts of a proton of Pro-2 and the C-3 and C-5 protons of Tyr-23, both residues located close to the termini in the crystal structure. The two remaining carbonyl titration shifts assigned to nonionizable amino acids do not experience a double titration reflected about the mid-pH range. This may indicate either that the acid and base conformations of residues near the termini are not completely identical or that another acid pH conformational change occurs elsewhere within the molecule. Peak 17 may correspond to Tyr-23 C^{α}, near the termini sensing the conformational change at low pH; peak 31 may represent the same C^{α} sensing its own titration and/or the conformational change at high pH.

Comparison of Computed $pK_{1/2}$ and Observed pK Values. Table V lists the ionizable groups of BPTI, the atom of each to which the charge was assigned, intrinsic pK values, and calculated static accessibilities used in the electrostatic computations. Tables I–IV list computed $pK_{1/2}$ values with experimentally determined pK values for all titrations from pH 2 to 12.[3] The two glutamic acid residues exhibit similar observed pK values as would be predicted from the nearly equivalent $pK_{1/2}$ values. Asp-50, which forms a salt bridge with Arg-53 in the crystal structure, has a $pK_{1/2}$ value much less than that of Asp-3, but this difference appears to be attenuated in the observed pK values of the solution structure.[4] The elevated $pK_{1/2}$ of Lys-41 relative to Lys-15, -26, and -46, all of which have nearly equivalent $pK_{1/2}$ values, corresponds

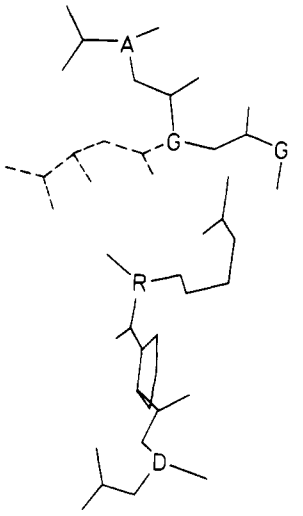

FIGURE 6: Part of the crystallographic structure of BPTI, showing the three residues at each terminus: Arg-1, Pro-2, Asp-3, and Gly-56, Gly-57, Ala-58, respectively. The position of the α carbon of each residue (with the exception of that of Pro-2) is marked by a single letter code for the appropriate amino acid. The hypothetical alteration in the C-terminal region taken as structure **10** is shown with broken lines.

well with the observed pK values. Although Tyr-23 was not expected to titrate due to its low static accessibility (0.10), it does exhibit deprotonation, having the highest observed pK value. Tyr-35 titrates with a greater observed pK value than Tyr-21 in agreement with the computed $pK_{1/2}$ values. The equivalent $pK_{1/2}$ values of Tyr-10 and -21 disagree with the significantly lower observed pK of Tyr-10 relative to Tyr-21 which has also been reported previously (Wagner & Wüthrich, 1975; Snyder et al., 1975). The α-amino and α-carboxyl pK values will be discussed below in relation to the proposed conformational change at the termini.

Discrepancies are in general likely attributable to crystal-solution conformational changes or effects of unconsidered perturbing forces (Botelho & Gurd, 1978; Gurd & Rothgeb, 1979). In the absence of major conformational changes, purely electrostatic effects will cause the pK of each ionizable group in a protein to vary with pH in such a way that each titration should exhibit negatively cooperative character, i.e., a Hill coefficient less than unity. Fitting the ^{13}C NMR data to the Hill equation (Markley & Finkenstadt, 1975) and allowing the slope to vary (i) did significantly improve (F test, $P = 0.1$) the fit to the data, (ii) did not change the observed pK values or acid and base limits significantly, and (iii) yielded Hill coefficients $\simeq 0.9$.[5]

Electrostatically Driven Conformational Change. The hypothetical structural transition of the COOH-terminal region resulting in the formation of the interterminal salt bridge has been described under Methods. The transition decreases the interterminal distance, $r_{N_1O_{58}}$, from 6.6 Å in the high-pH crystal conformation to 2.6 Å in the proposed salt-bridged conformation (see Figure 6). Table VI gives results of electrostatic computations at pH 6.0, $I = 0.10$, and selected $r_{N_1O_{58}}$. The interterminal electrostatic free energy, $\Delta G_{N_1O_{58},el}$, is listed with the magnitudes of net interaction of each of the termini with all charges of the protein except the opposite terminus, $\sum_{j\neq O_{58}} \Delta G_{N_1 j,el}$ (for N_1) and $\sum_{j\neq N_1} \Delta G_{O_{58} j,el}$ (for O_{58}), and the overall ΔG_{el} associated with N_1 and O_{58} is shown as the sum

[3] The standard deviations reported for the observed pK values in Tables I–IV were calculated by the computer program and were found to describe adequately the internal precision of the experiment. Only knowledge of the precision is necessary for comparing the differences between the individual observed pK values with those between the corresponding individual $pK_{1/2}$ values, since by the nature of the experiment each pK value is obtained under nearly identical conditions of observation.

[4] When the criterion that donor–acceptor distance be less than 3.1 Å is utilized, none of these residues are listed by Deisenhofer & Steigemann (1975) as participating in hydrogen bonds with uncharged groups and thus all are assigned normal pK_{int} values (Table V). Nevertheless, Asp-3, Glu-7, and Glu-49 each lie within 3.3 Å of uncharged groups with proton-donating capability and can be considered as participating in hydrogen bonds of slightly less strength. It is interesting to note that if the pK_{int} values are uniformly lowered by about 0.5 unit to take this into account, the calculated $pK_{1/2}$ values agree more closely with the observed pK values in addition to agreeing with their rank order.

[5] Tables I–IV show the results calculated with unit slope. Figures 2–5, parts B, were plotted according to variable slope calculations fitted to the numerous observed points.

Table VI: Electrostatic and Hydrophobic Free Energies and Terminal $pK_{1/2}$ Values for Initial BPTI and Selected Modified Structures, pH 6.0, I = 0.10 M

	structure				
	1	7	8	9	10
$r_{N_1O_{58}}$ (Å)	6.6	5.4	4.4	3.2	2.6
$\Delta G_{N_1O_{58},el}$ (kcal/mol)	−0.05	−0.17	−0.37	−0.87	−1.26
$\Sigma_{j\neq O_{58}}\Delta G_{N_1 j,el}$ (kcal/mol)	0.15	0.17	0.21	0.25	0.34
$\Sigma_{j\neq N_1}\Delta G_{O_{58}j,el}$ (kcal/mol)	−0.04	−0.09	−0.11	−0.16	−0.14
overall ΔG_{el} for N_1,O_{58} (kcal/mol)	0.06	−0.09	−0.27	−0.78	−1.06
$\delta\Sigma$AB (Å^2)	0	−23.2	−34.8	−55.5	−62.2
$\delta\Sigma\Delta G_H$ (kcal/mol)	0	−0.56	−0.84	−1.33	−1.49
$\delta\Sigma\Delta G_{el}$ (kcal/mol)	0	−0.15	−0.33	−0.84	−1.12
$\delta\Sigma(\Delta G_{el} + \Delta G_H)$ (kcal/mol)	0	−0.71	−1.17	−2.17	−2.61
$pK_{1/2}$(α-NH_2)	7.56[a]	7.64	7.75	8.07	8.28[c]
$pK_{1/2}$(α-COOH)	3.49[b]	3.37	3.20	2.80	2.57[d]

[a] This calculated $pK_{1/2}$ value = $-\log K_{2B}$ for use in eq 4. [b] This calculated $pK_{1/2}$ value = $-\log K_{2A}$ for use in eq 4. [c] This calculated $pK_{1/2}$ value = $-\log K_{1B}$ for use in eq 4. [d] This calculated $pK_{1/2}$ value = $-\log K_{1A}$ for use in eq 4.

of the above three energies. The corresponding contribution of the hydrophobic free energy to the conformational stability of each structure was calculated by the equation $\Delta G_H = -(24$ kcal mol^{-1} Å^{-2})AB where AB is the area buried (Å^2) (Chothia, 1974; Chothia & Janin, 1975). The differences between each altered structure and the high-pH crystal conformation are expressed as $\delta\Delta Q$ where Q is the quantity of interest found in Table VI.

In the salt-bridged conformation of Figure 6 the static accessibility of both termini is decreased relative to the high-pH crystal conformation. The stabilizing interaction is partially offset by increased electrostatic interaction with the rest of the protein to the extent of a net destabilization of +200 cal/mol (Table VI). This result is accounted for primarily by a net destabilization of +240 cal/mol between the termini and the Arg-1 guanidinium group. The overall $\delta\sum\Delta G_{el}$ between structures **1** and **10** is found to be −1.12 kcal/mol.

Table VI further lists the predicted $pK_{1/2}$ values for the α-amino and α-carboxyl groups, at I = 0.10 for structures **1** and **7**–**10**. Little significant change is observed prior to structure **7**, and after the termini have approached to the minimum distance of 2.6 Å in structure **10**, continued bond rotations result in approximately isoenergetic interaction. From eq 4 it may be seen that pK_{obsd} must lie between the pK_1 and pK_2 values of conformations 1 and 2, respectively, in Scheme I. Accordingly, it appears that the conformational transition may be assumed to progress beyond structure **8** to **9** or **10** in order to explain the pK_{obsd} values of 3.1 and 7.9 for the respective termini.

Under the assumption that structure **10** or an equivalent represents conformation 1, then the equilibrium constant K_3, between the dually charged conformations, HP(1) and HP(2), is calculated by using eq 4. Substitution of K_{1B}, K_{2B}, and $K_{obsd,B}$ for the α-amino group yields K_{3B} = 2.0, and substitution of K_{1A}, K_{2A}, and $K_{obsd,A}$ from the α-carboxyl group yields K_{3A} = 2.1. The agreement between these two values supports the implicit assumption of Scheme I that the acid-range conformation 2 is equivalent to the alkaline conformation 2, i.e., $K_{3A} = K_{3B} = K_3$. If this were not true, a general scheme similar to that of Bechet & D'Albis (1969), of which Scheme I is a special case, would be required to allow for differing acid and alkaline limiting conformations.

The K_{3A} and K_{3B} values further suggest that HP(1) is stabilized relative to HP(2) by a net free energy, ΔG_3, of approximately −0.43 kcal/mol. The ΔG_3 value may be divided into components as $\Delta G_3 = \delta\Delta G_{el} + \delta\Delta G_{conf}$, where $\delta\Delta G_{conf}$ is the nonelectrostatic free-energy difference between the two conformations. $\delta\Delta G_{conf}$ in turn may be considered as including $\delta\Delta G_H$, the hydrophobic free-energy change, and $\delta\Delta G_{CE}$, the change in energy due to conformational entropy reduction upon apposition of the termini. Substitution for all values estimated (Table VI) for the change from structure **1** to structure **10** gives an estimated $\delta\Delta G_{CE}$ of +2.11 kcal/mol, corresponding to a loss of about 7 eu.

The lack of appreciable cooperativity in the observed titration curves is compatible with the underlying hypothesis that this is a two-state system. However, if the potential well as determined by the oppositely directed enthalpic and entropic tendencies has a broad minimum, the states of the termini might be best described as sampling a range of isoenergetic conformations. The observation of large titration shifts for the terminal peaks 15 and 29 (Figure 3; Table II) when changing protonation state in comparison with the titration shifts seen when only changing conformation, as in the cotitrations, supports the model assumption that conformational effects upon the chemical shifts are small compared to the protonation effects.

Electrostatic Free Energies in BPTI. The summed stability for the native structure, ΔG_{el}, is plotted against pH, for I = 0.00 and 0.01, as curves A and B, respectively, in Figure 7. The extreme of about −2.5 kcal/mol lies near the protein isoelectric point, which is projected from the computed titration curve as pH 10.7, comparing closely with the experimental value pH 10.5 (Chauvet et al., 1964). The negative sign of the net free energy persists for much of the pH range below this point, into regions where the net charge nears +11.

The electrostatic stability will be significantly enhanced throughout the range of pH by the formation of the interterminal salt bridge, as indicated by curve C in Figure 7.

A notable role in the net stabilization of the molecule over the entire pH range is played by the nonuniform distribution of static accessibility, SA, values among the charge loci. Residues in electrostatically favorable environments tend to have lower SA. The effect of nonuniform SA is seen by a consideration of curve D in Figure 7. Curve D is that predicted for the hypothetical system in which all charge loci are assigned SA = 0.76, the average for all groups ionized at physiological pH. This system is clearly unstable relative to the others plotted in Figure 7. With the exception of the tyrosine groups, the most buried and therefore important sites are Arg-53 (SA = 0.30) and Asp-50 (SA = 0.35), interacting in the only salt bridge in the crystal structure, and Arg-20 (SA = 0.50) and Glu-7 (SA = 0.55). By use of the crystal coordinates, the salt bridge between residues 50 and 53 is calculated to be stabi-

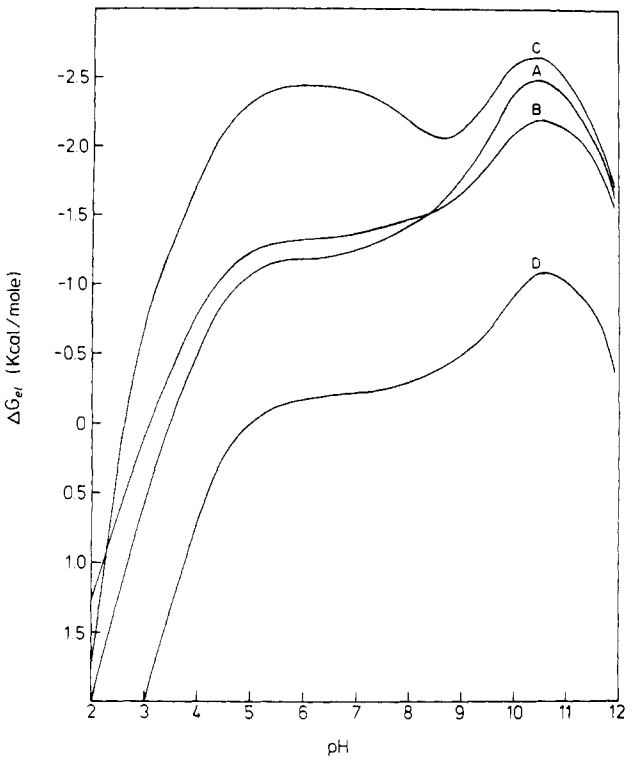

FIGURE 7: Dependence upon pH of summed electrostatic free energies in kilocalories per mole is shown for the native BPTI structure at I = 0.00 in curve A and I = 0.01 in curve B. Curve C shows the significantly broadened region of stability calculated for structure **10**. Curve D applies to a hypothetical system at I = 0.00 in which all SA values are set to 0.76. For clarity the curves for I = 0.10 are omitted.

lizing by 1.5 kcal/mol. Although the Arg-53 and Asp-50 charges should be strongly sensed throughout the molecule because of their low SA, the pair has little net effect upon other groups due to their mutual charge cancellation. The stabilization of the Arg-53 charge in this salt bridge may explain its singular resistance to modification despite extended treatment with the guanidinium selective reagent, phenylglyoxal (Keil, 1971).

Glu-7 is the most strongly interacting stabilizer for many groups, providing a stabilizing total of −770 cal/mol at pH 7, I = 0.00, whereas Arg-20 maximally destabilizes several groups, giving a total $\Delta G_{i,el}$ of +550 cal/mol. Well-defined interactions occur between Glu-7 and Lys-41 ($\Delta G_{7,41,el}$ = −350 cal/mol) and between Arg-20 and Lys-46 ($\Delta G_{20,46,el}$ = +360 cal/mol). Interestingly, the effects of specific modifications upon inhibitor activity implicate Glu-7 as the only carboxylate serving an essential structural role (Vincent et al., 1971).

Wagner et al. (1979) have investigated the changes in the thermal stability of BPTI upon selective reduction of the Cys-14–Cys-39 disulfide bond followed by protection of the cysteinyl side chains with groups bearing negative, neutral, and positive charge. Net stabilization of about 0.4 kcal/mol resulted from introduction of the two negative charges into the positive protein environment, whereas a destabilization of nearly 1.0 kcal/mol occurred upon the addition of two positive charges. Although this disulfide bond is located in an exposed position, the strength of these interactions suggests that the charged protecting groups may be partially inaccessible to solvent.

Conclusion. The modified Tanford–Kirkwood theory adequately describes differences in electrostatic environments of acidic and basic residues through the computed $pK_{1/2}$ as evidenced by comparison to differences between pK_{obsd} values (Tables I–IV). The formation of a salt bridge between the α-amino group and the α-carboxyl group at mid-pH values is consistent with (i) the observation of a conformational change by ^{13}C NMR, (ii) the combination of a structural transition model and the electrostatic theory, and (iii) the observed pK values for the termini. The electrostatic interactions are modulated by a distribution of static accessibilities which yield a negative ΔG_{el} and stabilize the folded form. The net electrostatic stabilization of the folded form presumably allows formation of the disulfide bridges under physiological conditions (Creighton, 1978) despite the presence of 11 positive charges and only 5 negative charges at neutral pH. The electrostatic stability of the crystal structure of BPTI, which is particularly adapted to high pH, is substantially increased in the pH range 3–9 by adoption of the interterminal salt bridge.

Electrostatic interactions within the trypsin system are currently being characterized and their effects upon conformation and activity evaluated. The present work is also being extended to an investigation of the electrostatic contribution to association of BPTI with trypsin, particularly considering the implications of the significant dipole calculated for BPTI.

Acknowledgments

Helpful discussions with Dr. J. B. Matthew, Dr. G. I. H. Hanania, and M. A. Flanagan are gratefully acknowledged. R. Addleman and D. Osman provided assistance with the NMR experiments and W. Morrow with computations. Thanks are also due to L. Steiger and John Hodges for help in preparing the manuscript and to Dr. J. Deisenhofer for advice and discussions.

Supplementary Material Available

Description of the structural transition model and expanded Tables Ia–IVa containing pentapeptide pK and chemical shift values as well as literature chemical shift values for titrating BPTI resonances (9 pages). Ordering information is given on any current masthead page.

References

Bechet, J.-J., & D'Albis, A. (1969) *Biochim. Biophys. Acta 178*, 561–576.

Bernstein, F. C., Koetzle, T. F., Williams, G. J. B., Meyer, E. F., Jr., Brice, M. D., Rodgers, J. R., Kennard, O., Shimanouchi, T., & Tasumi, M. (1977) *J. Mol. Biol. 112*, 535–542.

Botelho, L. H., & Gurd, F. R. N. (1978) *Biochemistry 17*, 5188–5196.

Botelho, L. H., Friend, S. H., Matthew, J. B., Lehman, L. D., Hanania, G. I. H., & Gurd, F. R. N. (1978) *Biochemistry 17*, 5197–5205.

Brown, H. K., & Gurd, F. R. N. (1981) *Pept., Proc. Am. Pept. Symp., 7th*, 123–126.

Brown, L. R., DeMarco, A., Wagner, G., & Wüthrich, K. (1976) *Eur. J. Biochem. 62*, 103–107.

Brown, L. R., DeMarco, A., Richarz, R., Wagner, G., & Wüthrich, K. (1978) *Eur. J. Biochem. 88*, 87–95.

Campbell, I. D., Dobson, C. M., Williams, R. J. P., & Xavier, A. V. (1973) *J. Magn. Reson. 11*, 172–181.

Chauvet, J., Nouvel, G., & Acher, R. (1964) *Biochim. Biophys. Acta 92*, 200–201.

Chothia, C. (1974) *Nature (London) 248*, 338–339.

Chothia, C., & Janin, J. (1975) *Nature (London) 256*, 705–708.

Cohn, E. J., & Edsall, J. T. (1943) *Proteins, Amino Acids and Peptides*, Chapter 4, Reinhold, New York.

Creighton, T. E. (1978) *Prog. Biophys. Mol. Biol. 33*, 231–298.
Deisenhofer, J., & Steigemann, W. (1975) *Acta Crystallogr., Sect. B B31*, 238–250.
Ernst, R. R., & Anderson, W. A. (1966) *Rev. Sci. Instrum. 37*, 93–102.
Flanagan, M. A., Ackers, G. K., Matthew, J. B., Hanania, G. I. H., & Gurd, F. R. N. (1981) *Biochemistry 20*, 7439–7449.
Friend, S. H., & Gurd, F. R. N. (1979a) *Biochemistry 18*, 4612–4619.
Friend, S. H., & Gurd, F. R. N. (1979b) *Biochemistry 18*, 4620–4630.
Friend, S. H., March, K. L., Hanania, G. I. H., & Gurd, F. R. N. (1980) *Biochemistry 19*, 3039–3047.
Friend, S. H., Matthew, J. B., & Gurd, F. R. N. (1981) *Biochemistry 20*, 580–586.
Gurd, F. R. N., & Rothgeb, T. M. (1979) *Adv. Protein Chem. 33*, 73–165.
Gurd, F. R. N., Keim, P., Glushko, V. G., Lawson, P. J., Marshall, R. C., Nigen, A. M., & Vigna, R. A. (1972) *Chemistry and Biology of Peptides*, pp 45–49, Ann Arbor Science Publishers, Inc., Ann Arbor, MI.
Harina, B. M., Dyckes, D. F., Willcott, M. R., III, & Jones, W. C. (1980) *J. Am. Chem. Soc. 102*, 1120–1124.
Huber, R., Kukla, O., Ruhlmann, A., Epp, O., & Formanek, H. (1970) *Naturwissenschaften 57*, 389–392.
Kassell, B., & Laskowski, M., Sr. (1965) *Biochem. Biophys. Res. Commun. 20*, 463–468.
Keil, B. (1971) *FEBS Lett. 14*, 181–184.
Keim, P., Vigna, R. A., Marshall, R. C., & Gurd, F. R. N. (1973a) *J. Biol. Chem. 248*, 6104–6113.
Keim, P., Vigna, R. A., Morrow, J. S., Marshall, R. C., & Gurd, F. R. N. (1973b) *J. Biol. Chem. 248*, 7811–7818.
Keim, P., Vigna, R. A., Nigen, A. M., Morrow, J. S., & Gurd, F. R. N. (1974) *J. Biol. Chem. 249*, 4149–4156.
Kuhlman, K. F., & Grant, D. M. (1971) *J. Chem. Phys. 55*, 2998–3007.
Lee, B. K., & Richards, F. M. (1971) *J. Mol. Biol. 55*, 379–400.
Maigret, B., Pullman, B., & Dreyfus, M. (1970) *J. Theor. Biol. 26*, 321–333.
Markley, J. L., & Finkenstadt, W. R. (1975) *Biochemistry 14*, 3562–3566.
Masson, A., & Wüthrich, K. (1973) *FEBS Lett. 31*, 114–118.
Matthew, J. B., & Richards, F. M. (1982) *Biochemistry* (in press).
Matthew, J. B., Hanania, G. I. H., & Gurd, F. R. N. (1978a) *Biochem. Biophys. Res. Commun. 81*, 410–415.
Matthew, J. B., Friend, S. H., Botelho, L. H., Lehman, L. D., Hanania, G. I. H., & Gurd, F. R. N. (1978b) *Biochem. Biophys. Res. Commun. 81*, 41–421.
Matthew, J. B., Hanania, G. I. H., & Gurd, F. R. N. (1979a) *Biochemistry 18*, 1919–1928.
Matthew, J. B., Hanania, G. I. H., & Gurd, F. R. N. (1979b) *Biochemistry 18*, 1928–1936.
Matthew, J. B., Friend, S. H., & Gurd, F. R. N. (1981) *Biochemistry 20*, 571–586.
Matthew, J. B., Friend, S. H., & Gurd, F. R. N. (1982) in *Interaction between Iron and Proteins in Oxygen and Electron Transport* (Ho, C., Ed.) Elsevier/North-Holland, New York (in press).
Maurer, W., Haar, W., & Ruterjans, H. (1974) *Z. Phys. Chem. (Wiesbaden) 93*, 119–129.
McCammon, J. A., Gelin, B. R., & Karplus, M. (1977) *Nature (London) 267*, 585–590.
Meloun, B., Fric, I., & Sorm, F. (1968) *Eur. J. Biochem. 4*, 112–117.
Norton, R. S., Clouse, A. O., Addleman, R. E., & Allerhand, A. (1977) *J. Am. Chem. Soc. 99*, 79–83.
Oldfield, E., Norton, R. S., & Allerhand, A. (1975) *J. Biol. Chem. 250*, 6381–6402.
Ramachandran, G. N., & Sasekharan, V. (1968) *Adv. Protein Chem. 23*, 283–438.
Richarz, R., & Wüthrich, K. (1978) *Biochemistry 17*, 2263–2269.
Russu, I. M., Ho, N. T., & Ho, C. (1980) *Biochemistry 19*, 1043–1052.
Sampson, P. F. (1970) *BMDX85*, UCLA Computer Center, Los Angeles, CA.
Scholtan, N., & Rosenkranz, H. (1966) *Makromol. Chem. 99*, 254–274.
Sherman, M. P., & Kassell, B. (1968) *Biochemistry 7*, 3634–3641.
Shire, S. J., Hanania, G. I. H., & Gurd, F. R. N. (1974a) *Biochemistry 13*, 2967–2974.
Shire, S. J., Hanania, G. I. H., & Gurd, F. R. N. (1974b) *Biochemistry 13*, 2974–2979.
Shire, S. J., Hanania, G. I. H., & Gurd, F. R. N. (1975) *Biochemistry 14*, 1352–1358.
Snyder, G. H., Rowan, R., III, Karplus, S., & Sykes, B. D. (1975) *Biochemistry 14*, 3765–3777.
Tanford, C., & Kirkwood, J. G. (1957) *J. Am. Chem. Soc. 79*, 5333–5339.
Vincent, J., Chicheportiche, R., & Lazdunski, M. (1971) *Eur. J. Biochem. 23*, 401–411.
Wagner, G., & Wüthrich, K. (1975) *J. Magn. Reson. 20*, 435–445.
Wagner, G., & Wüthrich, K. (1978) *Nature (London) 275*, 247–248.
Wagner, G., Kalb (Gilboa), A. J., & Wüthrich, K. (1979) *Eur. J. Biochem. 95*, 249–253.
Wenkert, E., Clouse, A. O., Cochran, D. W., & Doddrell, D. (1969) *J. Am. Chem. Soc. 91*, 6879–6880.